Somatotopy of cervical dystonia in motor-cerebellar networks: Evidence from resting state fMRI

Giuseppe A Zito, Clément Tarrano, Prasanthi Jegatheesan, Asya Ekmen, Benoît Béranger, Michael Rebsamen, Cécile Hubsch, Sophie Sangla, Cécilia Bonnet, Cécile Delorme, et al.

Somatotopy of Cervical Dystonia in motor-cerebellar networks: evidence from resting state functional connectivity

Running title: Resting state fMRI in Cervical Dystonia

Giuseppe A. Zito, PhD[1], Clement Tarrano MD[1], Prasanthi Jegatheesan, PhD[1], Asya Ekmen, MD[1], Benoît Béranger, MSc[2], Michael Rebsamen, MSc[3], Cécile Hubsch, MD, PhD[1], Sophie Sangla, MD[1], Cécilia Bonnet, MD PhD[1], Cécile Delorme, MD[1], Aurélie Méneret, MD, PhD[1], Bertrand Degos, MD, PhD[1], Floriane Bouquet, MD[1], Marion Apoil Brissard, MD[5], Marie Vidailhet, MD, Cécile Gallea, PhD[1§], Emmanuel Roze, MD PhD[1§], Yulia Worbe, MD PhD[1,6§]

§ - These authors contributed equally to the work

[1] Sorbonne University, Inserm U1127, CNRS UMR7225, UM75, Paris Brain Institute, Movement Investigation and Therapeutics Team, Assistance Publique – Hôpitaux de Paris, DMU Neurosciences, Paris, France

[2] Center for NeuroImaging Research (CENIR), Paris Brain Institute, Sorbonne University, UPMC Univ Paris 06, Inserm U1127, CNRS UMR 7225, Paris, France

[3] Support Centre for Advanced Neuroimaging (SCAN), University Institute of Diagnostic and Interventional Neuroradiology, Inselspital, Bern University Hospital, University of Bern, Freiburgstrasse, Bern, CH-3010, CH

[4] Université de Caen Normandie, Caen, France

[6] Department of Neurophysiology, Saint-Antoine Hospital, Assistance Publique - Hôpitaux de Paris, Paris, FR

*** Correspondence:**

Prof. Emmanuel Roze
Salpêtrière Hospital
47-83 Boulevard de l'Hôpital, 75013 Paris, France
Email : emmanuel.flamand-roze@aphp.fr

Word count: 2731

Keywords: Cervical dystonia, resting state fMRI, motor cortex, cerebellum

Financial disclosure: This work was supported by the Swiss National Science Foundation (P400PM_183958), AMADYS, Fondation Brou de Laurière, Merz-Pharma. This project was also supported by « Agence Nationale de la Recherche (ANR) » under the frame of the European Joint Programme on Rare Diseases (EJP RD, ANR-16-CE37-0003-03).

The authors declare no conflict of interest.

Abstract

Background

Cervical dystonia is the most frequent form of isolated focal dystonia. It is often associated with a dysfunction in brain networks, mostly affecting the basal ganglia, the cerebellum, and the somatosensory cortex. However, it is unclear if such a dysfunction is somato-specific to the brain areas containing the representation of the affected body part, and may thereby account for the focal expression of cervical dystonia.

In this study, we investigated resting state functional connectivity in the areas within the motor cortex and the cerebellum containing affected and non-affected body representation in cervical dystonia patients.

Methods

Eighteen patients affected by cervical dystonia and 21 healthy controls had resting state fMRI. The functional connectivity between the motor cortex and the cerebellum, as well as their corresponding measures of gray matter volume and cortical thickness, were compared between groups. We performed seed-based analyses, selecting the different body representation areas in the precentral gyrus as seed regions, and all cerebellar areas as target regions.

Results

Compared to controls, patients exhibited increased functional connectivity between the bilateral trunk representation area of the motor cortex and the cerebellar vermis 6 and 7b, respectively. These functional abnormalities did not correlate with structural changes or symptom severity.

Conclusions

Our findings indicate that the abnormal function of the motor network is somato-specific to the areas encompassing the neck representation. Functional abnormalities in discrete relevant areas of the motor network could thus contribute to the focal expression of CD.

Introduction

Cervical dystonia (CD) is the most common form of isolated focal dystonia, characterized by involuntary muscle contractions in the neck, which results in abnormal head posture and movements.[1] It has been associated with various brain dysfunctions, such as maladaptive neuroplasticity, abnormal sensorimotor processing and integration,[2] and its pathophysiological mechanisms are still unclear.[3]

CD is considered a network disorder arising from abnormal communication among different brain areas.[2] Neuroimaging studies have evidenced functional and structural abnormalities in the basal ganglia,[2, 4] the sensorimotor and frontoparietal regions, the insula, the cerebellum, and the brainstem.[5-7] Animal and human research indicate that both the cerebello-thalamo-cortical network and basal ganglia–thalamo-cortical network project into the motor cortex, where the motor output is generated,[8] and may contribute to the abnormal movements.[9] Other studies focusing on the cerebellum have reported loss of Purkinje cells, areas of focal gliosis,[10] as well as increased gray matter (GM) volume of cerebellar flocculus, in CD patients compared to healthy controls (HC).[11] Altogether, these findings point to the motor cortex and the cerebellum as critical structures for the pathogenesis of CD.

It is mostly unknown whether these network abnormalities represent a general marker of the pathogenesis of dystonia, irrespectively of the affected body part, or if the pathogenesis of different types of dystonia affects relevant discrete areas within the motor areas and cerebellum. Distinct patterns of altered microstructures within regions of basal ganglia and cerebellar circuits have been associated with different phenotypes of focal dystonia,[12] and regional patterns of functional connectivity within the striatum and a sensorimotor-parietal network, as opposed to global network dysfunction, may contribute to focal dystonia.[13, 14] So far, there is no detailed study of the cerebellar somatotopy in CD, since a high-definition functional cerebellar atlas has been developed only recently.[15] Such an investigation is not trivial, as it has been shown that the representations of multiple body parts are organized in an orderly manner in the cerebellar lobes, mirroring the functional specialization of the motor cortex.[15, 16]

In this study, we investigated the specificity of motor-cerebellar networks in CD using resting state functional connectivity (RS-FC). RS-FC is a widely used non-invasive technique, based on functional magnetic resonance imaging (fMRI), where the time courses of predefined regions of interest (ROIs) are extracted from the brain at rest, and correlated with each other, under the assumption that functionally connected areas show high correlation.[17] We compared patterns of RS-FC in the different body representation areas of the motor cortex and the cerebellum between patients affected by CD and

HC, and performed a morphometric analysis on the same areas to study differences in GM volumes and cortical thickness (CT) between groups. We tested the hypothesis that network dysfunctions in CD are somato-specific, i.e., CD patients exhibit abnormal RS-FC and structural differences only in the head and neck representation areas, in both the motor cortex and the cerebellum.

Materials and Methods

Subjects and general procedure

We recruited 18 CD patients (7 male, mean age=46.9±8.7 years) and 21 sex- and age-matched HC (9 male, mean age=45.3±10.6 years). Patients were recruited at the Pitié-Salpêtrière Hospital, Paris, FR. Inclusion criteria for patients were: a diagnosis of CD, no botulin toxic injection within 3 months prior to the examination, and stable pharmacological treatment in the month preceding inclusion. Exclusion criteria common to both HC and CD patients were: i) any other neurological sign, and ii) incompatibility with MR acquisition. Severity of CD was assessed at the time of inclusion with the Toronto Western Spasmodic Torticollis Rating Scale (TWSTRS), subscale for severity.[18] Between-group differences in age were assessed with independent-sample t-tests, whereas differences in the ratio between male and female participants were assessed with χ^2 tests.

The study was carried out in accordance with the latest version of the Declaration of Helsinki and approved by the local Ethics Committee (approval number: C17-04 - AU 1360, ClinicalTrial.gov ID: NCT03351218). All participants gave written informed consent prior to the study.

Neuroimaging acquisition parameters and pre-processing

During the MR session, participants lied in the scanner while fixating a cross displayed on a screen. Their gaze was monitored with eye-tracking. Neuroimaging data were acquired using a 3T Magnetom Prisma (Siemens, DE) with a 64-channel head coil. Resting state fMRI and structural images were acquired in one session. Structural images were acquired with a T1-weighted MP2RAGE sequence with Repetition Time (TR)=5 s, Inversion Time (TI)=700/2500 ms, field of view (FOV)=232×256 in plane ×176 slices, 1 mm isotropic, Ipat acceleration factor=3. FMRI data were acquired with an echo-planar imaging (EPI) sequence performed with a multi-slice, multi-echo acquisition, TR=1.9 s, Echo Time (TE)=17.2/36.62/56.04 ms, Ipat acceleration factor=2, Multi-band=2, isotropic voxel size=3 mm,

dimensions=66×66 in plane ×46 slices, 350 volumes, duration=11 min. The first 10 time points were not recorded to ensure magnetization equilibrium.

Image preprocessing was done as follows: structural images were background denoised[19, 20] in order to improve the quality of the subsequent steps, segmented and normalized to the Montreal Neurological Institute (MNI) space using the Computational Anatomy Toolbox (CAT12)[21] extension for SPM12.[22] Functional images were pre-processed according to standard pipelines (despiking, slice timing correction and realignment to the volume with the minimum outlier fraction driven by the first echo) using AFNI.[23] A brain mask was computed on the realigned shortest echo temporal mean using FSL BET[24] in order to increase the robustness against signal bias intensity. Afterwards, the TEDANA toolbox[25] version 0.0.7 was used to optimally combine the realigned echoes, to apply principal component analysis and reduce the dimensionality of the data, and to perform an independent component analysis (ICA) decomposition to separate BOLD and non-BOLD components.[26] This step ensured robust artefact removal of non-BOLD signals, such as movement, respiration or heartbeat, and has already shown to be superior over standard denoising techniques in regressing out motion.[25] Framewise displacement (FD) was further computed according to standard methods,[27] and compared between CD patients and HC. The quality of the signal was verified as head movement amplitude was minimal, and the FD did not statistically differ between CD patients (0.018±0.016 mm) and HC (0.016±0.008 mm) [$t(37)=0.49$, $p=0.629$]. Finally, using SPM12, functional images were co-registered to the T1-weighted image, normalized to MNI space, and smoothed with a Gaussian kernel with full width at half maximum of 4x4x4 mm, as previously suggested.[28]

After pre-processing, the CONN toolbox[29] implemented in Matlab r2018a (The MathWorks Inc. USA) was used to parcellate the brain images into 274 functional regions, based on the Brainnetome Atlas,[28] and to extract the region-averaged time series. Motion parameters obtained during the realignment, as well as the average signal of white matter and cerebrospinal fluid obtained during the segmentation, were regressed out with aCompCor.[30] This step reduced spatial correlations resulting from physiological noise. Time series were finally band-pass filtered at $0.01<f<0.1$ Hz, according to previous research.[28]

Analysis of resting state functional connectivity

We entered all the time series extracted from the 274 functional regions into a first level general linear model (GLM), where we performed a ROI-based analysis, for each participant, to determine significant

resting state connections at individual level: In particular, we used bivariate correlation coefficients between all pairs of ROIs as indicators of their functional connectivity. Next, we converted the correlation coefficients to z-scores using Fisher-Z transformation, in order to normalize them to a Gaussian distribution. We then implemented a second level GLM testing seed-based ROI-to-ROI differences between CD and HC. For the latter, as we were only interested in the connectivity between the motor cortex and the cerebellum, we isolated the regions of the Brainnetome Atlas that were associated with the body representation areas within the precentral gyrus (PrG) and paracentral lobule (PCL), as well as all cerebellar regions without a priori, i.e. irrespective of body representation (Table 1). We then selected the bilateral motor areas as seed ROIs and the cerebellar ROIs as target regions. False positive control for multiple comparisons was implemented using false discovery rate (FDR)-corrected p-values with a threshold of $p_{FDR}<0.050$.

A correlation analysis was performed by computing Pearson correlation's coefficients between the severity of dystonia (TWSTRS scores) and the connectivity values between the motor cortex and the cerebellum. A FDR-corrected threshold of $p_{FDR}<0.050$ was applied.

Table 1. List of seed and target ROIs used in the analysis of functional connectivity. The Brainnetome Atlas was used to isolate all regions associated with the body representation areas within the motor cortex, as well as all cerebellar regions. R = right, L = left, PrG = precentral gyrus. PCL = paracentral lobule.

Seed regions (Motor cortex)	**MNI coordinates (x,y,z)**	**Target regions (Cerebellum)**	**MNI coordinates (x,y,z)**
R / L PrG, area 4 (head and face region)	R: 55, -2, 33 L: -49, -8, 39	R / L Lobules 1, 2, 3, 4	R: 10 -43 -18 L: -7 -44 -17
R / L PrG, caudal dorsolateral area 6	R: 33, -7, 57 L: -32, -9, 58	R / L Lobule 5	R: 14 -51 -19 L: -13 -50 -19
R / L PrG, area 4 (upper limb region)	R: 34, -19, 59 L: -26, -25, 63	R / L Lobule 6	R: 24 -58 -25 L: -23 -59 -25
R / L PrG, area 4 (trunk region, including neck)	R: 15, -22, 71 L : 15, -22, 71	R / L Lobule 7b	R: 28 -66 -51 L: -26 -66 -51
R / L PrG, area 4 (tongue and larynx region)	R : 54, 4, 9 L: -52, 0, 8	R / L Lobule 8a	R: 26 -58 -53 L: -24 -57 -53

R / L PrG, caudal ventrolateral area 6	R: 51, 7, 30 L: -49, 5, 30	R / L Lobule 8b	R: 18 -51 -55 L: -17 -50 -55
R / L PCL, areas 1, 2, 3 (lower limb region)	R: 10, -34, 54 L: -8, -38, 58	R / L Lobule 9	R: 7 -53 -49 L: -7 -53 -48
R / L PCL, area 4 (lower limb region)	R: 5, -21, 61 L: -4, -23, 61	R / L Lobule 10	R: 22 -37 -46 L: -21 -37 -45
		R / L Crus 1	R: 38 -68 -32 L: -36 -68 -32
		R / L Crus 2	R: 26 -76 -41 L: -26 -75 -42
		Vermis 6	1 -70 -21
		Vermis / Crus 1	-4 -78 -27
		Vermis / Crus 2	1 -75 -31
		Vermis 7b	0 -68 -31
		Vermis 8a	0 -67 -38
		Vermis 8b	0 -63 -42
		Vermis 9	0 -56 -37
		Vermis 10	1 -48 -35

Analysis of structural data

We performed a morphometric analysis to study differences in GM volume between CD patients and HC. After preprocessing, the normalized GM volumes obtained during the segmentation were smoothed using a 4 mm full breadth at half maximum kernel, in line with our functional analysis. Volumes from the ROIs in the motor cortex were extracted with CAT12[21] using the "ROI tool" option, whereas volumes in the cerebellar ROIs were extracted with the Spatially Unbiased Infratentorial toolbox (SUIT).[31] For the latter, we first isolated the infratentorial structures using *suit_isolate_seg*, we then performed an affine alignment to the specific SUIT template and applied a normalisation using *suit_normalize_dartel*, and finally we extracted the GM volumes using *suit_reslice_dartel*.

We also studied differences in CT between patients and controls, by extracting CT in the investigated ROIs with DL+DiReCT.[32] This method already showed high accuracy compared to standard instruments.[32] Due to the lack of available tools to reliably measure CT in the cerebellum, this analysis was performed only for the somatotopic regions of the motor cortex.

The extracted GM volumes and CTs were compared between groups with independent-sample t-tests implemented in SPSS 25 (IBM Inc., USA). A threshold of $p<0.050$ was selected.

Results

No significant differences were found in age and sex ratio between male and female participants (Table 2). CD patients showed symptom severity of 18.3 ± 4.4, as assessed with the TWSTRS.

Table 2. Clinical and demographic information. Comparison of clinical and demographic scores between groups. TWSTRS = Toronto Western Spasmodic Torticollis Rating Scale, HC = healthy controls, CD = cervical dystonia,

	HC (N = 21)	**CD (N = 18)**	**Statistics**
Sex [male / female]	9 / 12	7 / 11	$\chi(1) = 0.06$, $p = 0.802$
Age [years, mean ± SD]	45.3 ± 10.6	46.9 ± 8.7	$t(37) = 0.53$, $p = 0.600$
TWSTRS	-	18.3 ± 4.4	-
Overall medication [N (% of CD)]	-	18 (100%)	
- Botox [N (% of TD)]*	-	17 (94.4%)	
- Others (Tramadol, Levothyroxine, Diazepam, Escitalopram – [N (% of CD)])	-	3 (16.7%)	

* last Botox injection administered at least 3 months prior to the experiment.

Resting state functional connectivity and structural analysis

The analysis of RS-FC revealed increased functional connectivity, in CD patients compared to HC, of the bilateral trunk representation area 4 (PrG) with the cerebellar Vermis 6 [$F(2,36)=10.78$, $p_{FDR}=0.039$]

and Vermis 7b [$F(2,36)=10.33$, $p_{FDR}=0.039$], respectively (Figure 1). Detailed values of RS-FC in the two groups are displayed in Figure 2. No significant differences in the connectivity between the other seed ROIs and the cerebellum (Table 1) were found across groups ($p_{FDR}>0.050$ – Supplementary Figure 1).

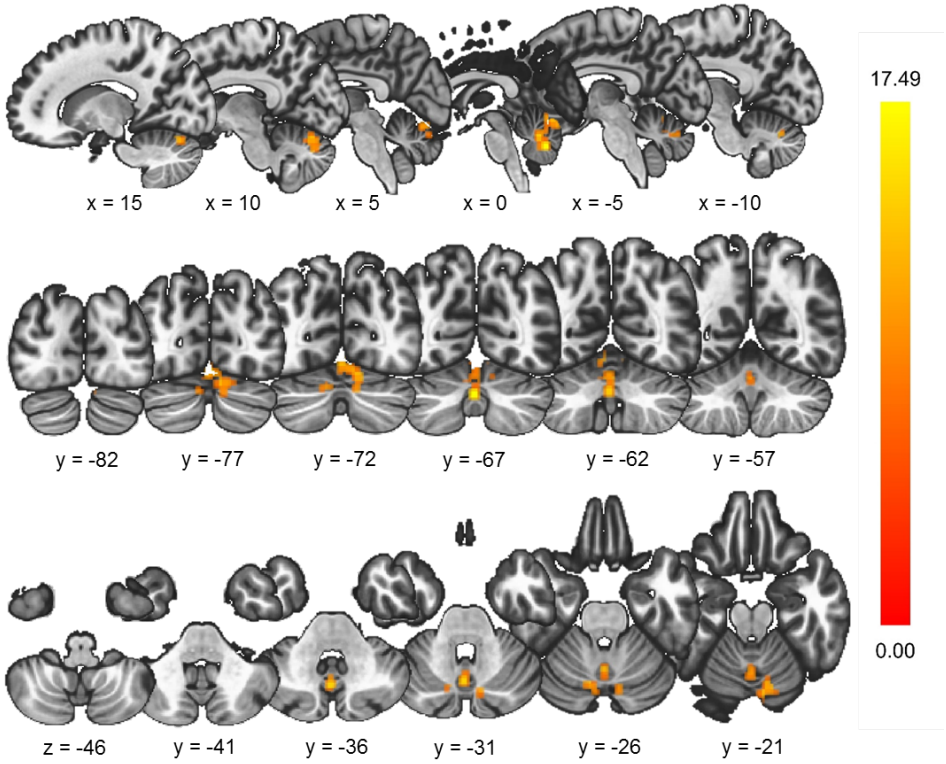

Figure 1. Between-group differences in the connectivity of the bilateral trunk representation area 4 of the PrG (seed) with the cerebellar Vermis 6 and 7b (target). Color bar represents the F-values assessed with the general linear model. For visualization purposes, the significant connectivity values are displayed irrespectively of the cerebellar ROIs.

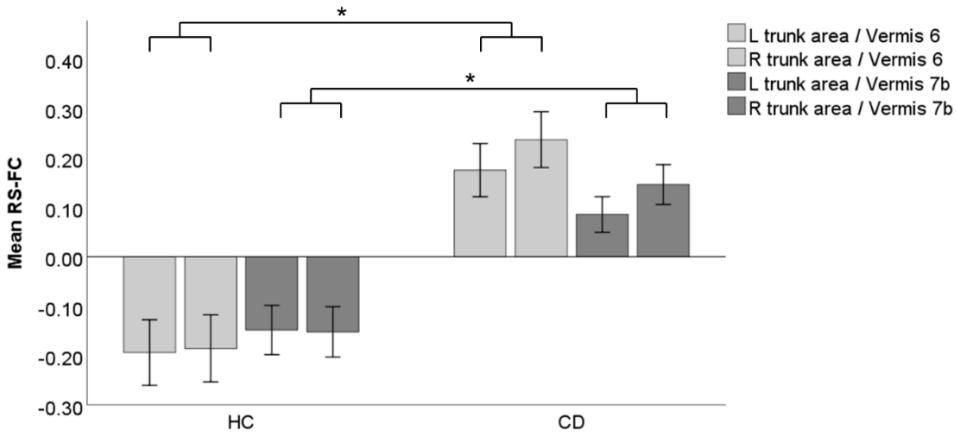

Figure 2. Mean values of resting state functional connectivity between ROIs. Error bars represent the standard error of the mean. * depicts significant differences (p_{FDR}<0.050) between CD patients and HC.

No correlation was found between any of the investigated connections and symptoms' severity in CD (p_{FDR}>0.050). Neither differences in GM volume, nor in CT, were found between the studied groups, in any of the investigated ROIs (p>0.050).

Discussion

Compared to HC, patients with CD showed increased RS-FC between the neck and trunk representation in area 4 of the precentral gyrus (PrG) and the cerebellar Vermis 6 and 7b. This pattern was neither associated with differences in GM volumes or CT between groups, nor with symptoms' severity in CD. Our findings indicate that the abnormal function of the motor network is somato-specific to the areas encompassing the neck and trunk representation. Functional abnormalities in discrete relevant areas of the motor network could thus contribute to the focal expression of CD.

The use of resting state fMRI was a strength of this study, as it allowed us to investigate task-free patterns of functional connectivity, hence, to avoid a potential bias due to adaptive/compensatory processes associated with task execution. This is relevant, as dystonic symptoms tend to worsen during voluntary motor activity, and compensatory mechanisms are more likely to occur during task execution than rest.[33] However, neuroimaging analyses can hardly distinguish causes from effects, therefore the causal mechanisms here discussed are speculative.

The cerebellum is of particular importance for the pathophysiology of CD, as the topographical expression of dystonia depends on the extent of cerebellar dysfunction in a dedicated mouse model.[34]

In this model, a dysfunction of the entire cerebellum induces a phenotype similar to generalized dystonia, whereas dysfunctions in limited cerebellar regions restrict abnormal movements to isolated body parts, like in focal dystonia. Hence, the extent, but not the location of the cerebellar dysfunction, seems to be linked to the severity of dystonia. Altered connectivity between the cerebellum and the sensorimotor areas has also been associated with the pathogenesis of CD.[3, 35, 36] However, reported changes were not limited to the somatotopic representation of the affected body parts,[3, 37, 38] and the potential link between critical areas within these regions and the location of dystonic manifestations is still poorly understood. Our results challenge this view, and provide evidence of well-defined regions in both the precentral gyrus (PrG) and the cerebellum specifically relevant to the clinical expression of CD, namely the trunk representation area 4 of the PrG and the cerebellar Vermis 6 and 7b. No other areas within the PrG and the cerebellum showed any group differences in RS-FC between patients and HC, thereby reinforcing the hypothesis of a selective area, with a critical role in motor control of head and neck, responsible for the pathogenesis of CD. More specifically, the trunk representation area 4 of the PrG contains neuronal populations responsible for the sternocleidomastoid muscle,[39, 40] typically affected in CD. Likewise, the cerebellar Vermis 6 has been related to saccadic eye movements in healthy subjects,[41, 42] and clinical studies have confirmed a link between abnormal cerebellar output and an impairment in saccadic adaptation,[43] vestibule-ocular reflex,[44] and eye-hand coordination[45] in CD. This may reflect cerebellar-related maladaptive plasticity associated with an attempt to compensate the abnormal head posture with a modulation of eye movements.[46, 47]

Abnormal connectivity of brain networks linking the cerebellum and the motor cortex has been largely investigated for its role in the pathogenesis of dystonia.[4] In non-human primates[48] and mice,[34] dystonic movements can be provoked by manipulations of the cerebellum, abnormal firing of the Purkinje cells has been found in DYT1 torsin1-knock-in mice,[49] and acute knock-down of Sgce in the cerebellum produces motor symptoms close to myoclonus dystonia in mice.[50] In humans, abnormal anatomical cerebello-thalamo-cortical connectivity can play a role in the clinical expression of dystonia,[51] as well as in the loss of cerebellar control over sensorimotor plasticity.[52] CD patients with a sensory trick show a differential ability to modulate the connectivity of the sensorimotor network, likely through a cerebellar mediation,[36] and modulation of the cerebello-cortical connectivity has been associated with the clinical improvement following botulinum toxin injections in these patients.[53]

We hypothesize that the abnormal connectivity between the motor cortex and the cerebellum found in our study reflects a cerebellar dysfunction mediating sensorimotor integration and maladaptive plasticity. This interpretation is consistent with the head neural integrator model,[54, 55] by which changes in any of the inputs of the integrator affect the communication between the cerebellum and cortical areas, and potentially lead to the manifestation of CD.[7, 56] In healthy subjects, proprioceptive input from the neck can substantially change the way cerebellar output influences plasticity at the level of the motor cortex,[57] and in CD, an abnormal integration of the neck proprioceptive information could drive an atypical functioning of the integrator,[57] which may generate head twists. The specific involvement of Vermis 6 and 7b found in our study provides further insights into the role of cerebellar areas associated with saccadic eye movements in the integrator dysfunction of CD.[11, 46]

The investigated differences in functional connectivity were not associated with structural changes in CD, as evidenced by our analysis of GM volume and CT, and this supports the vision that CD mainly affects brain functions. Research on this topic has shown controversial results, and while the classic assumption is that CD is not associated with structural changes in the brain,[58] some studies have reported altered GM concentration in CD patients in the cerebellar flocculus, as well as in the basal ganglia, the thalamus and the motor cortex.[11, 59] Such differences from our findings may be explained by different methodological approaches: While the previously used whole-brain approaches have identified differences in various structures, regardless of their functional roles, we focused on areas associated with specific functions relevant for CD, such as neck movements, and therefore opted for a ROI approach, which grouped together voxels belonging to the same functional areas. Even though our choice may have been more conservative than other approaches, it suggests that CD-related brain dysfunctions are not linked to structural changes. Future research should further investigate this topic, for instance by applying multimodal imaging techniques or ultra-high field MR, which could reveal subtle structural changes undetectable with conventional MRI.

In conclusion, our results point to an impairment in the communication of somato-specific cerebello-cortical networks related to head position and saccadic eye movements.[4] This impairment might be the consequence of abnormal processing of proprioceptive input from the neck, which affects the functioning of the head neural integrator, and in turn generates abnormal head posture, as well as related compensatory eye movements.

Acknowledgements

The Authors would like to acknowledge the Swiss National Science Foundation (SNSF), the Paris Brain Institute, and the University Hospitals Pitié-Salpêtrière for the support. We would also like to thank all the participants of our study.

Authors' roles

Research project. Conception and organization: ER, YW. Execution: CT, AE, CH, SS, CB, CD, AM, BD, FB, MAB, PJ.

Statistical analysis. Design and execution: GAZ, CG, BB, MR, YW. Review and critique: GAZ, CG, BB, MR, ER, YW.

Manuscript. Writing of the first draft: GAZ, YW. Review and critique: GAZ, CG, BB, MR, CT, AE, CH, SS, AMB, CD, AM, BD, FB, MAB, PJ, ER, YW.

Full financial disclosure

The authors declare no conflict of interest. GAZ is supported by the Swiss National Science Foundation (SNSF, grant number P400PM_183958). AH is supported by the AFSGT. BB is supported by the Paris Brain Institute. JF is supported by the "Investissements d'avenir" ANR-10-IAIHU-06, the ICM Big Brain Theory Program (project PredictICD) and the Inria Project Lab Program (project Neuromarkers). AM received a travel grant from Merz. ER served on scientific advisory boards for Orkyn, Aguettant, Merz-Pharma, Allergan; received honoraria for speeches from Orkyn, Aguettant, Merz-Pharma, Everpharma, International Parkinson and Movement disorders Society; received research support from Merz-Pharma, Orkyn, Aguettant, Elivie, Ipsen, Allergan, Everpharma, Fondation Desmarest, AMADYS, Fonds de Dotation Brou de Laurière, Agence Nationale de la Recherche, Societé Française de Médecine Esthétique; received travel grant from Vitalaire, PEPS development, Aguettant, Merz-Pharma, Ipsen, Merck, Orkyn, Elivie, Adelia Medical, Dystonia Medical Research Foundation, International Parkinson and Movement disorders Society, European Academy of Neurology, International Association of Parkinsonism and Related Disorders. MV received honorarium from MDS and EAN and grants/research support from patient's associations (tremor, APTES; dystonia, Dystonia Coalition and AMADYS, PSP France, France Parkinson) and research foundation FRM (Medical Research Foundation). Y. Worbe received research support from Agence Nationale de la Recherche,

Dystonia Medical Research Foundation and Fondation de France; and has received travel grants from Merz-Pharma and the European Society for study for Tourette Syndrome.

References

1. Geyer HL, Bressman SB. The diagnosis of dystonia. The Lancet Neurology 2006;5(9):780-790.
2. Quartarone A, Hallett M. Emerging concepts in the physiological basis of dystonia. Movement Disorders 2013;28(7):958-967.
3. Burciu RG, Hess CW, Coombes SA, et al. Functional activity of the sensorimotor cortex and cerebellum relates to cervical dystonia symptoms. Human brain mapping 2017;38(9):4563-4573.
4. Prudente CN, Hess EJ, Jinnah H. Dystonia as a network disorder: what is the role of the cerebellum? Neuroscience 2014;260:23-35.
5. de Vries PM, Johnson KA, de Jong BM, et al. Changed patterns of cerebral activation related to clinically normal hand movement in cervical dystonia. Clinical neurology and neurosurgery 2008;110(2):120-128.
6. Battistella G, Termsarasab P, Ramdhani RA, Fuertinger S, Simonyan K. Isolated focal dystonia as a disorder of large-scale functional networks. Cerebral cortex 2015;27(2):bhv313.
7. Sedov A, Popov V, Shabalov V, Raeva S, Jinnah H, Shaikh AG. Physiology of midbrain head movement neurons in cervical dystonia. Movement Disorders 2017;32(6):904-912.
8. Bostan AC, Strick PL. The cerebellum and basal ganglia are interconnected. Neuropsychology review 2010;20(3):261-270.
9. Filip P, Gallea C, Lehéricy S, et al. Disruption in cerebellar and basal ganglia networks during a visuospatial task in cervical dystonia. Movement Disorders 2017;32(5):757-768.
10. Prudente C, Pardo C, Xiao J, et al. Neuropathology of cervical dystonia. Experimental neurology 2013;241:95-104.
11. Draganski B, Thun-Hohenstein C, Bogdahn U, Winkler J, May A. “Motor circuit” gray matter changes in idiopathic cervical dystonia. Neurology 2003;61(9):1228-1231.
12. Berman BD, Honce JM, Shelton E, Sillau SH, Nagae LM. Isolated focal dystonia phenotypes are associated with distinct patterns of altered microstructure. NeuroImage: Clinical 2018;19:805-812.
13. Teive HA, Chen CC. Isolated focal dystonia: The mysterious pathophysiology is being unraveled. AAN Enterprises; 2020.
14. Norris SA, Morris AE, Campbell MC, et al. Regional, not global, functional connectivity contributes to isolated focal dystonia. Neurology 2020;95(16):e2246-e2258.
15. Boillat Y, Bazin P-L, van der Zwaag W. Whole-body somatotopic maps in the cerebellum revealed with 7T fMRI. Neuroimage 2020;211:116624.
16. Mottolese C, Richard N, Harquel S, Szathmari A, Sirigu A, Desmurget M. Mapping motor representations in the human cerebellum. Brain 2013;136(1):330-342.
17. Friston K, Frith C, Liddle P, Frackowiak R. Functional connectivity: the principal-component analysis of large (PET) data sets. Journal of Cerebral Blood Flow & Metabolism 1993;13(1):5-14.
18. Consky E, Basinski A, Belle L, Ranawaya R, Lang A. The Toronto Western Spasmodic Torticollis Rating Scale (TWSTRS): assessment of validity and inter-rater reliability. Neurology 1990;40(suppl 1):445.
19. O'Brien KR, Kober T, Hagmann P, et al. Robust T1-weighted structural brain imaging and morphometry at 7T using MP2RAGE. PloS one 2014;9(6).
20. Marques J.
21. A Computational Anatomy Toolbox for SPM.
22. Statistical Parametric Mapping.
23. Analysis of Functional NeuroImages.
24. Jenkinson M, Beckmann CF, Behrens TE, Woolrich MW, Smith SM. Fsl. Neuroimage 2012;62(2):782-790.
25. Kundu P, Voon V, Balchandani P, Lombardo MV, Poser BA, Bandettini PA. Multi-echo fMRI: a review of applications in fMRI denoising and analysis of BOLD signals. Neuroimage 2017;154:59-80.
26. Kundu P, Inati SJ, Evans JW, Luh W-M, Bandettini PA. Differentiating BOLD and non-BOLD signals in fMRI time series using multi-echo EPI. Neuroimage 2012;60(3):1759-1770.
27. Power JD, Mitra A, Laumann TO, Snyder AZ, Schlaggar BL, Petersen SE. Methods to detect, characterize, and remove motion artifact in resting state fMRI. Neuroimage 2014;84:320-341.

28. Fan L, Li H, Zhuo J, et al. The human brainnetome atlas: a new brain atlas based on connectional architecture. Cerebral cortex 2016;26(8):3508-3526.
29. Whitfield-Gabrieli S, Nieto-Castanon A. Conn: a functional connectivity toolbox for correlated and anticorrelated brain networks. Brain connectivity 2012;2(3):125-141.
30. Behzadi Y, Restom K, Liau J, Liu TT. A component based noise correction method (CompCor) for BOLD and perfusion based fMRI. Neuroimage 2007;37(1):90-101.
31. Diedrichsen J. A spatially unbiased atlas template of the human cerebellum. Neuroimage 2006;33(1):127-138.
32. Rebsamen M, Rummel C, Reyes M, Wiest R, McKinley R. Direct cortical thickness estimation using deep learning-based anatomy segmentation and cortex parcellation. Human brain mapping 2020;41(17):4804-4814.
33. Li Z, Prudente CN, Stilla R, Sathian K, Jinnah HA, Hu X. Alterations of resting-state fMRI measurements in individuals with cervical dystonia. Human brain mapping 2017;38(8):4098-4108.
34. Raike RS, Pizoli CE, Weisz C, van den Maagdenberg AM, Jinnah H, Hess EJ. Limited regional cerebellar dysfunction induces focal dystonia in mice. Neurobiology of disease 2013;49:200-210.
35. Lehéricy S, Tijssen MA, Vidailhet M, Kaji R, Meunier S. The anatomical basis of dystonia: current view using neuroimaging. Movement Disorders 2013;28(7):944-957.
36. Sarasso E, Agosta F, Piramide N, et al. Sensory trick phenomenon in cervical dystonia: a functional MRI study. Journal of neurology 2020;267(4):1103-1115.
37. Meunier S, Garnero L, Ducorps A, et al. Human brain mapping in dystonia reveals both endophenotypic traits and adaptive reorganization. Annals of Neurology: Official Journal of the American Neurological Association and the Child Neurology Society 2001;50(4):521-527.
38. Ramdhani RA, Kumar V, Velickovic M, Frucht SJ, Tagliati M, Simonyan K. What's special about task in dystonia? A voxel-based morphometry and diffusion weighted imaging study. Movement Disorders 2014;29(9):1141-1150.
39. Thompson M, Thickbroom G, Mastaglia F. Corticomotor representation of the sternocleidomastoid muscle. Brain: a journal of neurology 1997;120(2):245-255.
40. Prudente CN, Stilla R, Buetefisch CM, et al. Neural substrates for head movements in humans: a functional magnetic resonance imaging study. Journal of Neuroscience 2015;35(24):9163-9172.
41. Voogd J, Schraa-Tam CK, van der Geest JN, De Zeeuw CI. Visuomotor cerebellum in human and nonhuman primates. The Cerebellum 2012;11(2):392-410.
42. Park IS, Lee NJ. Roles of the Declive, Folium, and Tuber Cerebellar Vermian Lobules in Sportspeople. Journal of clinical neurology (Seoul, Korea) 2018;14(1):1.
43. Mahajan A, Gupta P, Jacobs J, et al. Impaired Saccade Adaptation in Tremor-Dominant Cervical Dystonia—Evidence for Maladaptive Cerebellum. The Cerebellum 2020:1-9.
44. Stell R, Bronstein A, Marsden C. Vestibulo-ocular abnormalities in spasmodic torticollis before and after botulinum toxin injections. Journal of Neurology, Neurosurgery & Psychiatry 1989;52(1):57-62.
45. Maurer C, Mergner T, Luecking C, Becker W. Adaptive changes of saccadic eye–head coordination resulting from altered head posture in torticollis spasmodicus. Brain 2001;124(2):413-426.
46. Bradnam L, Chen CS, Callahan R, Hoppe S, Rosenich E, Loetscher T. Visual compensation in cervical dystonia. Journal of clinical and experimental neuropsychology 2019;41(7):769-774.
47. Hirsig A, Barbey C, Schüpbach MW, Bargiotas P. Oculomotor functions in focal dystonias: A systematic review. Acta Neurologica Scandinavica 2020;141(5):359-367.
48. Wilson BK, Hess EJ. Animal models for dystonia. Movement Disorders 2013;28(7):982-989.
49. Liu Y, Xing H, Wilkes BJ, et al. The abnormal firing of Purkinje cells in the knockin mouse model of DYT1 dystonia. Brain Research Bulletin 2020;165:14-22.
50. Washburn S, Fremont R, Moreno-Escobar MC, Angueyra C, Khodakhah K. Acute cerebellar knockdown of Sgce reproduces salient features of myoclonus-dystonia (DYT11) in mice. Elife 2019;8:e52101.
51. Argyelan M, Carbon M, Niethammer M, et al. Cerebellothalamocortical connectivity regulates penetrance in dystonia. Journal of Neuroscience 2009;29(31):9740-9747.
52. Hubsch C, Roze E, Popa T, et al. Defective cerebellar control of cortical plasticity in writer's cramp. Brain 2013;136(7):2050-2062.
53. Hok P, Hvizdošová L, Otruba P, et al. Botulinum toxin injection changes resting state cerebellar connectivity in cervical dystonia. Scientific reports 2021;11(1):1-11.
54. Klier EM, Wang H, Constantin AG, Crawford JD. Midbrain control of three-dimensional head orientation. Science 2002;295(5558):1314-1316.

55. Sedov A, Semenova U, Usova S, et al. Implications of asymmetric neural activity patterns in the basal ganglia outflow in the integrative neural network model for cervical dystonia. Progress in brain research 2019;249:261-268.
56. Shaikh AG, Zee DS, Crawford JD, Jinnah HA. Cervical dystonia: a neural integrator disorder. Brain 2016;139(10):2590-2599.
57. Popa T, Hubsch C, James P, et al. Abnormal cerebellar processing of the neck proprioceptive information drives dysfunctions in cervical dystonia. Scientific reports 2018;8(1):1-10.
58. Gracien R-M, Petrov F, Hok P, et al. Multimodal quantitative MRI reveals no evidence for tissue pathology in idiopathic cervical dystonia. Frontiers in neurology 2019;10:914.
59. Obermann M, Yaldizli O, De Greiff A, et al. Morphometric changes of sensorimotor structures in focal dystonia. Movement disorders 2007;22(8):1117-1123.

Figures' captions

Figure 1. Between-group differences in the connectivity of the bilateral trunk representation area 4 of the PrG (seed) with the cerebellar Vermis 6 and 7b (target). Color bar represents the F-values assessed with the general linear model. For visualization purposes, the significant connectivity values are displayed irrespectively of the cerebellar ROIs.

Figure 2. Mean values of resting state functional connectivity between ROIs. Error bars represent the standard error of the mean. * depicts significant differences ($p_{FDR}<0.050$) between CD patients and HC.